J Mater Sci: Mater Med (2009) 20:2275–2284
DOI 10.1007/s10856-009-3797-y

Fabrication and characterization of chitosan coated braided PLLA wire using aligned electrospun fibers

Wen Hu · Zheng-Ming Huang · Shu-Yan Meng · Chuang-long He

Received: 29 October 2008 / Accepted: 2 June 2009 / Published online: 12 June 2009

Abstract The development of functionalized braided wires coated with chitosan that can be used for tissue suturing and tissue regeneration is the subject of this work. Poly(L-lactic acid) (PLLA) braided wires were successfully fabricated by combining an electrospinning technique and alignment collection with a mini-type braiding method. The resulting PLLA wires with and without chitosan coating were characterized through a variety of methods including scanning electron microscopy (SEM), X-ray photoelectronic spectra (XPS) and tensile mechanical testing. Hemolytic property, kinetic hemostasis behavior, platelet adhesion, erythrocyte adhesion, and water uptake ability of the wires were explored. The results showed that a nearly comparable mechanical behavior of the braided wires with some commercial suture could be obtained with well-aligned fibers, and no significant difference in tensile performances were recognized with and without the introduction of chitosan. The PLLA wires coated with chitosan were found to have better prohemostatic activity than those without a chitosan coating.

W. Hu
School of Materials Science and Engineering, Tongji University, 1239 Siping Road, Shanghai 200092, China

Z.-M. Huang (✉)
School of Aerospace Engineering and Applied Mechanics, Tongji University, 1239 Siping Road, Shanghai 200092, China
e-mail: huangzm@mail.tongji.edu.cn

S.-Y. Meng
Shanghai Pulmonary Hospital, 507 Zhengmin Road, Shanghai 200433, China

C. He
College of Chemistry, Chemical Engineering and Biotechnology, Donghua University, Shanghai 201620, China

1 Introduction

Sutures are primarily used in surgery to draw tissues together [1–4]. Successful wound healing depends on an appropriate tensile strength provided by the suture materials and a microenvironment in which the repaired tissues are likely to attach and grow. Although nonabsorbable sutures maintaining a persistent tension may facilitate wound healing [5, 6], people undertaking them cannot avoid the pain the second operation brought. On the other hand, absorbable sutures will eventually absorbed by human body and no second operation is required. Almost all of the sutures in the current usage only play one role, i.e., to mechanically tie wounded tissues together. They do not have an additional function such as to release a drug. However, when implanted in human body, sutures often provoke different levels of inflammatory response, resulting in susceptibility to Surgical Site Infection (SSI) [7]. Hybrid sutures with targeted physico-mechanical properties and biological activity will be highly preferred.

Ultrathin fibers with diameters ranging from submicrons to several nanometers, which are fabricated by an electrospinning technique and are called nanofibers for simplicity, have received tremendous attentions in biomedical fields in recent years [8, 9]. Electrospun nanofibers with pore sizes small enough to prevent the penetration of pathogenic microorganisms into a wound meet most of the requirements for preventing adhesion and growth of pathogenic microorganisms that can cause infection in the body. The high specific surface area of the electrospun materials is highly effective in terms of absorption of body fluids and promotes wound healing [10, 11]. Electrospun nanofibers were often collected in a random non-woven form, due to instability of charged jet and chaos of the jet path [12, 13]. Obtaining undirectionally aligned fibers with highly ordered structure

is necessary in some specific cases when the fiber mechanical performance is of a primary consideration.

In our previous report [14], a novel way to fabricate medical agent loaded fibrous threads using electrospun and aligned composite nanofibers was proposed. However, the mechanical strength of the threads was insufficient to meet the clinical requirements for a suture application. To overcome this problem, the present study made use of a braiding technique to combine multiple threads into a braided wire, which is better in structural integrity. Surface coating using chitosan was applied to the developed wire sutures. The application of surface coating to a suture material has a benefit of smoothing suture surface, combating bacterial colonization and enhancing certain other properties [7, 15]. Chitosan was seen to have an ability to initiate the hemostasis independently of platelets or coagulation factors [16–18]. A comparison study for the braided sutures with and without chitosan coating was carried out. Morphological features and mechanical properties of the sutures were characterized. Their blood compability and hemostasis behavior were explored. Animal tests to evaluate sutures knotting and suturing properties were also carried out in the paper.

2 Experimental part

2.1 Materials

PLLA (M_w = 100 000 g mol^{-1}) and chitosan (M_w = 100 000 g mol^{-1}, degree of deacetylation 80%) were purchased from AK Biotech Ltd, Shandong, China. Acetic acid and 2,2,2-trifluoroethanol (TFE) were obtained from Shanghai Chemical Agent Corporation (China), which were used as solvents for chitosan and PLLA, respectively. The reagents were all of analytical grade.

The PLLA was dissolved in TFE at room temperature and the solution was stirred for 2–3 h until it became homogenous to prepare the PLLA solution with a concentration of 8 wt% by weight.

To examine adhesion of blood cells (erythrocytes and platelets) on the PLLA sutures, fresh venous whole blood from a healthy volunteer, who had not taken any medication for at least 10 days, was drawn by venipuncture. The blood was taken in sodium citrate (3.13 wt%) at a blood/citrate ratio of 9/1 (v/v). $CaCl_2$ solution was used as a coagulant.

2.2 Electrospinning

An experimental setup for preparing aligned nanofibers is shown schematically in Fig. 1. It basically consists of a DC voltage generator (Beijing Machinery & Electricity Institute, China), a syringe pump (model WZ-50C2, Zhejiang

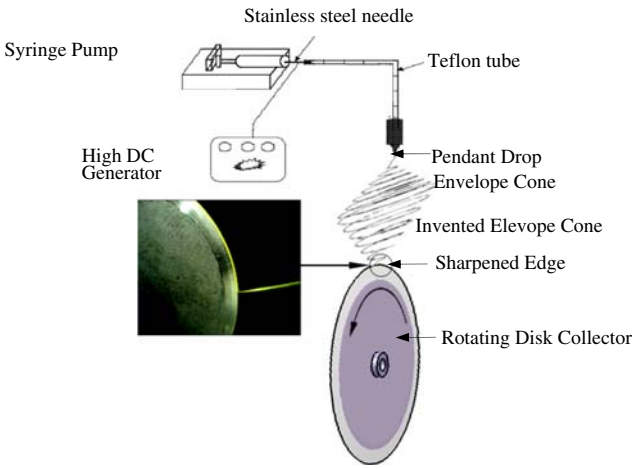

Fig. 1 Experimental setup for preparing aligned electrospun fibers used in this study

University's Medical Instrument Co., Ltd), a self-made spinneret system, and a grounded rotating edge-sharpened disc collector with a diameter of 280 mm and an optimal rotation speed of 1205 rpm which was the best collecting speed to collect the aligned fibers in the previous research. When the disc collector was used, the produced fibers were forced to deposit onto its sharp edge and would around the disc driven by a DC motor.

The tip-to-collector distance was set to 10 cm and the collecting time was 4 min. The electrospinning was done at an ambient temperature (25°C) with a humidity of 40–60%. The flow rate was adjusted to 3 ml h^{-1} and the electrical voltage was 25 kV.

2.3 Suture fabrication

The aligned fiber bundle with a diameter of about 0.078 mm (Fig. 2) was manually taken out from the edge of the

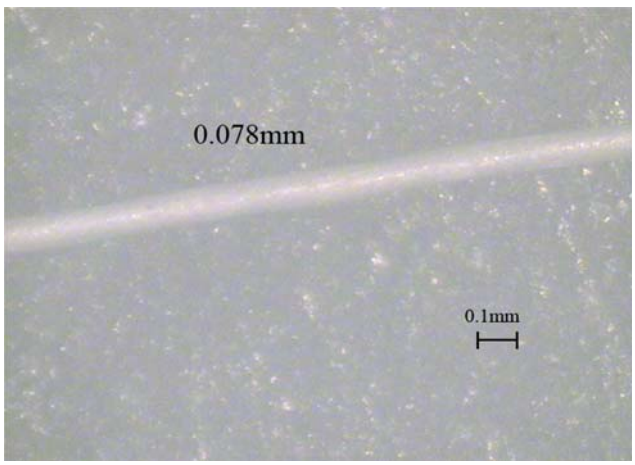

Fig. 2 Electrospun fiber bundle collected by a rotating disc

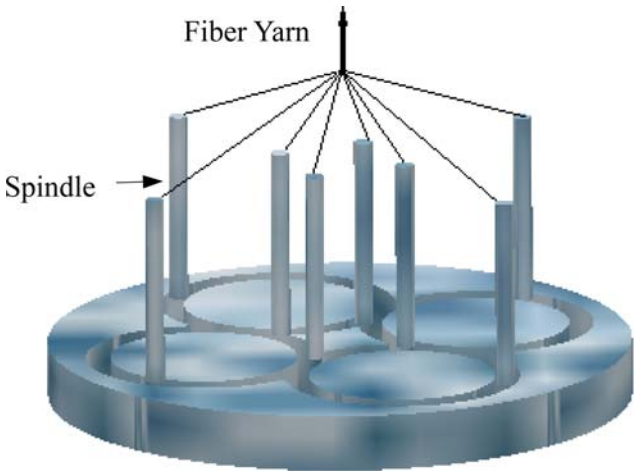

Fig. 3 Schematic of minitype braiding machine

Fig. 4 Optical microscope photograph of a braided wire

collector after sufficient fibers were collected (for 4 min). In order to eliminate internal stresses, the fiber bundles were transferred to a custom-made device for post-treatment, which is a combination of hot-stretching and twisting. After some trial and error, the best post-treatment condition consisted of a tension ratio of about 50% and a heating temperature of 80°C. In the treatment, the tensile force applied on the fiber bundle was kept for 2 h under 80°C, which would improve the fiber bundle size stability. Then, an even number of the fiber bundles with better mechanical performance was used to fabricate a braided wire through a minitype braiding machine (Fig. 3), giving a diameter of about 0.35 mm. In this way, a PLLA braided suture based on electrospun nanofibers was made successfully, as can be seen in Fig. 4.

2.4 Surface coating

Chitosan solution was prepared by dissolving it in a suitable amount of acetic acid at room temperature under magnetic stirring for 3 h. The resulting solution had a weight ratio of 1 wt%. The previously fabricated PLLA sutures were dipped into the chitosan solution and stirred for 30 min using magnetic stirring in order to ensure a complete penetration of chitosan into the pores of the PLLA sutures. After that, the chitosan coated PLLA sutures were washed three times with 0.1 M NaOH solution and with deionized water.

2.5 Morphological characterization

Morphology of the collected fibers was observed under an environmental scanning electron microscopy (ESEM, PHILIPS XL 30, Netherlands) with an accelerating voltage of 20 kV. The samples for SEM observation were sputter coated with gold. The fiber diameter of the electrospun fibers was measured through image visualization software ImageJ 1.34 s (National Institutes of Health, USA). The average fiber diameter and diameter distribution were determined from about 50–60 measurements of the random fibers upon a typical SEM image. The fibrous bundles and braided thread were examined by an optical microscope (Union D23, Olympus, Japan) equipped with a plus image capturing system. The captured images were analyzed through software ImageJ 1.34 s to determine diameters of the fiber bundles and braided threads. Five samples of each group of the threads were tested at three different equidistant points, and the mean diameter value for each kind of the threads was obtained from the average of the five sample measurements.

2.6 XPS analysis

Surface structures of the samples were examined using an X-ray photoelectron spectrometer (XPS: Kratos, XSAM800, Great Britain) with a monochromated Mg Ka (1253.6 eV) X-ray source. The measurements were carried out at a work power of 12 kV × 15 mV. Data acquisition was performed at a pressure of 2 × 107 Pa. A value of 284.8 eV of the hydrocarbon C1 s core level was used as calibration for the absolute energy scale.

2.7 Tensile test

Tensile properties of the PLLA sutures and the chitosan coated sutures were measured according to ASTM Standard D 2256-02 [19]. Before the measurement, the sutures were sufficiently dried in an oven of 80°for 2 h. Four to six specimens of each kind of the sutures were tensile tested on a small-size tester (Model CSS-44020, China) with a load cell of 200 N. Two metal pins of 8 mm diameter mounted perpendicularly to the actuator and load cell were used to secure the thread specimen (Fig. 5), leaving a gauge length of 13–15 cm. A cross-head speed

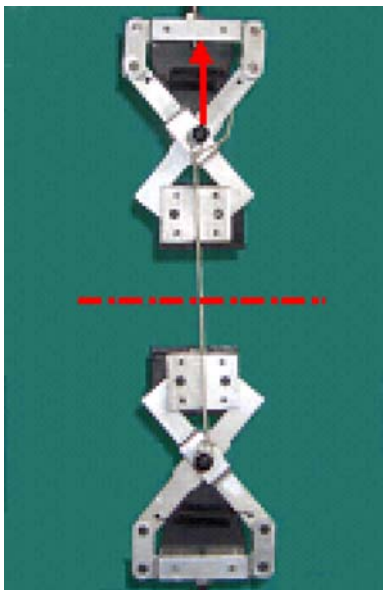

Fig. 5 Device for tensile testing

of 10 mm min^{-1} was applied during the test. For each specimen, the load versus cross-head displacement data from initial until rupture load levels was measured using a PC data acquisition system connected to the tester. Mean values together with standard deviations were calculated for all of the tested specimens.

2.8 Determination of hemolytic property

Hemolytic properties of the PLLA and PLLA-CS sutures were examined by spectrophotometry. Dilute blood for the examination was made by dispersing 8 ml of the volunteer's pure blood in 10 ml of physiological saline. Each suture sample, which has a mass of 1 g was put in a tube and was washed three times using distilled water, followed by rinsing another three times in physiological saline. Then, the sample was soaked in a fluid medium contained in the tube, which was put in a water bath at 37°C for 60 min. Three kinds of fluid media were used. They were the dilute blood made as aforementioned, a mixture solution of the 0.2 ml dilute blood with 10 ml physiological saline, and another mixture solution of the 0.2 ml dilute blood with 10 ml distilled water. For convenient description, these media are called medium *S*, medium *N*, and medium *P*, respectively.

After the sample was removed from the tube, the fluid medium was centrifuged at 1000 rpm for 5 min, and the supernatant liquid containing heme was collected to determine an absorbance at a wavelength of 545 nm. The absorbance was represented by A_S, A_N, or A_P if the fluid medium used was the medium *S*, medium *N*, or the medium *P*, respectively. With these definitions, a hemolytic ratio (HR) was given as follows:

$$\mathrm{HR} = \frac{A_S - A_N}{A_P - A_N} \times 100\%$$

If the calculated HR was greater than 5%, it means that the suture sample used was blood compatible.

2.9 Kinetic hemostasis experiment

The PLLA sutures and chitosan coated sutures were cut to 2 cm long segments. Each group of the suture segments were put on the concave surfaces of six watch glasses, which were placed in air for a few minutes. The six watch glasses, covered with the same suture samples, were injected with 0.2 ml volunteer's pure blood that had been anticoagulated with sodium citrate and 25 μl (0.2 mol/l) $CaCl_2$ solution. After the blood was mixed with $CaCl_2$ solution in the watch glasses, the time of blood coagulating was recorded using a stopwatch. In every 5 min, one of the watch glasses was immerged into a beaker containing 100 ml deionized water. The absorbency (A_S) of the water was measured at a wavelength of 545 nm using a spectrophotometer. Plain glass surfaces without any suture samples were also tested following the same procedure to obtain reference levels for the respective absorbency data. A parallel experiment for each sample was conducted three times. The blood anticoagulant index (BCI) versus time curves were plotted.

$$\mathrm{BCI} = \frac{A_S}{A_W} \times 100\%$$

where A_w was the absorbance of the solution in which 0.25 ml of the whole blood was mixed with 50 ml of physiological saline solution. If the curve descended rapidly, it meant that the suture under consideration had a good hemoglutination characteristic. In the contrast when the curve went downward slowly and lasted for a long period of time, the suture was said to exhibit a poor hemoglutination behavior.

2.10 Platelet adhesion

To understand platelet adhesion behavior, a suitable amount of the volunteer's pure blood was loaded into a tube, which was centrifuged at 1000 rpm for 15 min. The suspension was centrifuged at 1600 rpm for additional 15 min. Then, the supernatant within the second tube was removed, whereas the remaining was taken as platelet rich plasma (PRP). The suture samples, having a mass of 10 mg, were washed three times using deionized water and subsequently rinsed with 0.1 M phosphate buffer (PBS). The sutures were promptly introduced into the wells of 24-well tissue culture polystyrene plates and fixed to the well bottom using o-rings. The PRP was added onto the surface of each sample

and incubated at 37°C for 30 min. The samples were then washed with 0.1 M PBS three times to remove any unadhered platelets. The adhered platelets were fixed with 2% glutaraldehyde solution in 0.1 M PBS for 1 h. The samples were later washed again three times using 0.1 M PBS. Afterwards, they were dehydrated through a graded series of ethanol solutions for 10 min and further with 100% ethanol for additional 30 min, before being allowed to dry in air for at least 10 h. Finally, the samples were coated with gold in *vacuum*. The platelets on each sample were examined by scanning electron microscopy (ESEM, PHILIPS XL 30, Netherlands). The samples were tested in duplicate.

2.11 Erythrocyte adhesion

An erythrocyte adhesion experiment was carried out similarly as done a platelet adhesion test. The only difference was that for the erythrocyte adhesion test the suspension in the centrifuge tube was obtained by centrifugation at 800 rpm for 10 min, rather than at 1000 rpm for 15 min.

2.12 Determination of water uptake

Water uptake behavior of the sutures was studied by putting them in 25 ml phosphate buffer solution (pH 7.4) at 37°C for 4, 24, 48, 72, and 96 h, respectively. Before the experiment, all of the suture samples were tried completely under a vacuum evaporator for 24 h, followed by a balance treatment by placing the sutures at room temperature until no change in the suture weight was attained. The dry sutures were accurately weighed ($\sim$0.1 g) and immersed in the buffer solution. At predetermined time intervals (4, 24, 48, 72, and 96 h) the swollen sutures were taken out of the solution, wiped with tissue paper, and weighed. The degree of water uptake for each sample at time t was calculated by using an expression: $(W_t - W_0)/W_0 \times 100\%$, where W_t and W_0 were the masses of the sample at time t and in the dry state, respectively.

3 Results and discussion

3.1 Surface topography analysis

When a grounded rotating disk with a sharp edge was used to collect aligned electrospun fibers, the fiber alignment depends on rotating speed and other electrospinning parameters. Our previous study [14] have demonstrated that a higher rotating speed tended to give better fiber alignment as the speed was increased from 500 to 1200 rpm. However, a speed higher than 1300 rpm would result in a faster flow of air which may blow over the aligned fibers. An optimal rotation rate was found to be

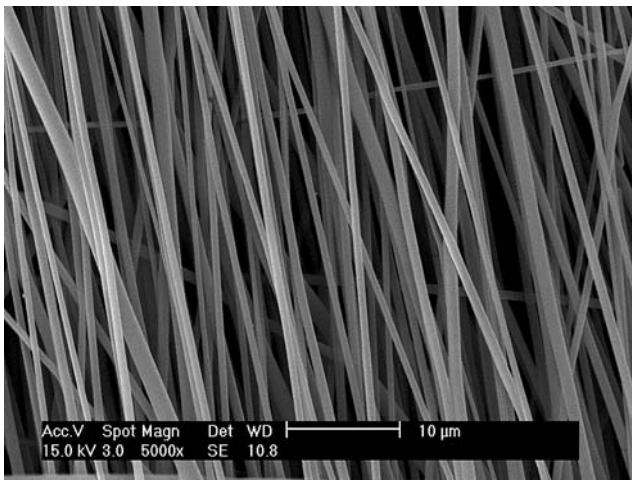

Fig. 6 Aligned electrospun fibers collected by a high speed rotating disc

1205 rpm, which was used in this study. SEM micrographs of the aligned fibers, taken from the rim of the disk, are shown in Fig. 6. It can be seen that the fibers made from PLLA solution with 8 wt% concentration had good topography, without any beads on the fiber surface. An averaged fiber diameter measured by image software image J 1.34 s was 667 nm. The collecting time, which, as can be imaged, has an intimate relationship with fiber bundle diameter, was chosen as 4 min. Too little time was difficult to collect enough fibers, whereas too much time would result in a fiber bundle with a too big diameter.

3.2 XPS analysis

XPS survey scan spectra analysis was used to characterize surface chemical composition of the pure PLLA (Fig. 7a) and PLLA-CS sutures (Fig. 7b), respectively. The XPS spectra indicated that C1s and O1s scan spectra appeared on the PLLA sample at binding energies of 286.6 and 532.8 eV (Fig. 7), respectively. No nitrogen peak was found in Fig. 7a. In the contrast, the PLLA-CS sample exhibited N1 s scan spectra in addition to C1s and O1s scan spectras at a binding energy of about 400 eV. Figure 7c gave the N1s narrow scan spectra of PLLA-CS suture, which were fitted according to the known binding energies of different nitrogen containing the groups. Two peaks occurred in Fig. 7c indicating that the PLLA-CS sample contained two nitrogen regions with binding energies of 400.37 and 398.49 eV which corresponded to the elements $-NHCOCH_3$ and $-NH_2$ of the coated chitosan, respectively [20]. The results of XPS confirm that chitosan has been successfully coated on the surface of the PLLA sutures since there are no nitrogen atoms in PLLA molecules. The chemical compositions of the PLLA and PLLA-CS samples calculated from the XPS survey scan spectra

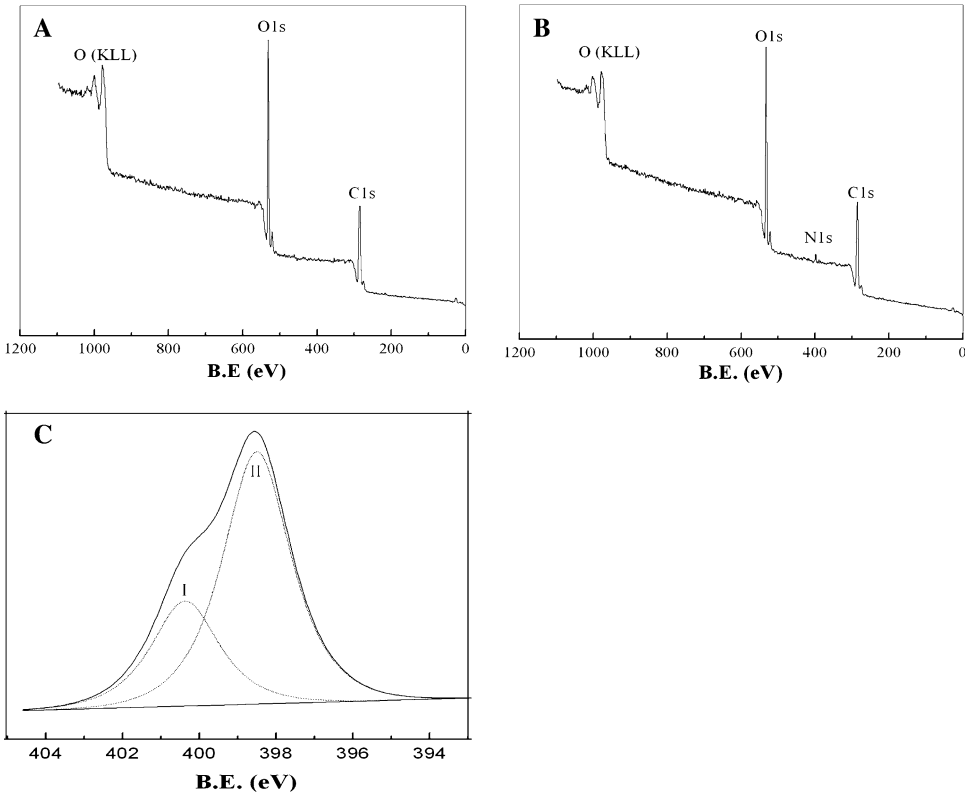

Fig. 7 XPS survey scan spectra of **a** pure PLLA, **b** PLLA-CS sutures, and **c** XPS N1s narrow scans with the curve fit of PLLA-CS sample

Table 1 Elemental composition of the samples

Sample	Composition (%)		
	C	N	O
PLLA	65.09	0.00	34.91
PLLA-CS	64.64	2.34	33.01

were shown in Table 1. Nitrogen content of the PLLA-CS determined by XPS was 2.34%, whereas carbon and oxygen content decreased a litte bit compared with pure PLLA. This could be attributed to the introduction of chitosan. A SEM image (Fig. 8, denoted by arrows) also confirmed that deposition of chitosan on the PLLA suture surface was achieved.

3.3 Tensile property

Tensile stress-strain curves of both the PLLA and PLLA-CS sutures were shown in Fig. 9. It can be seen that the curves essentially exhibited a bilinear behavior with an initial elastic segment followed by a plastic one. From the tensile curves, the mechanical properties of the sutures were obtained. These, together with averaged suture diameters, are listed in Table 2. The tensile breaking force is proportional to the suture size (diameter), which, in the present case, was directly related to a collecting time for aligned fibers. We chose 4 min as the collecting time and the diameter of braided sutures thus obtained was of about 0.35 ± 0.10 mm, which is comparable to the diameters of most commercial sutures. All of the braided suture samples

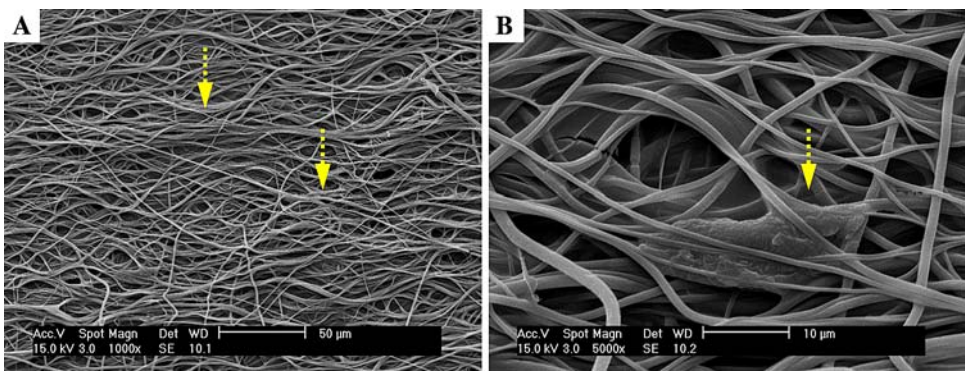

Fig. 8 SEM photograghs of braided PLLA nanofiber sutures coated with chitosan: **a** 1 k magnification, **b** 5 k magnification (chitosan deposition on nanofibers indicated by *arrow* points)

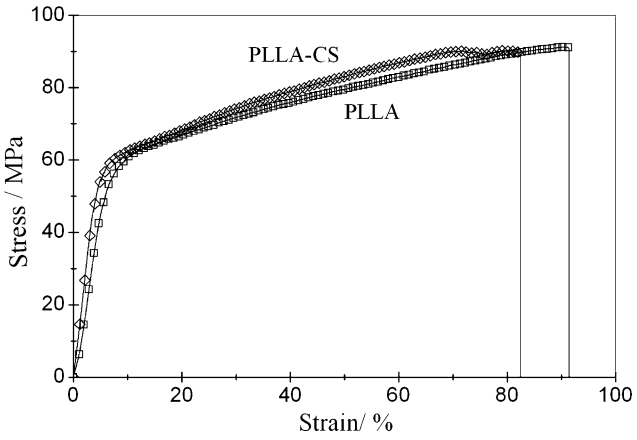

Fig. 9 Tensile stress-strain curves of PLLA and PLLA-CS sutures

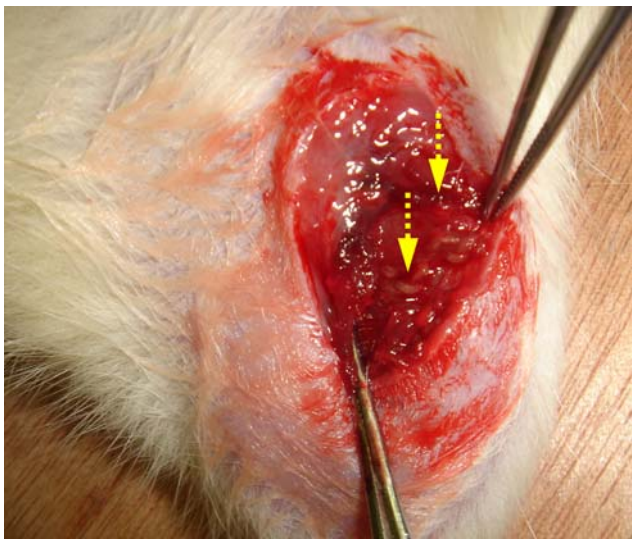

Fig. 10 Photo of a part of an animal implanted with PLLA-CS suture, in which arrows indicate the suture after 28 day implantation

showed a breaking force of around 8.8N, which is close to 10.2N required by a 2–0 type collagen suture with a diameter from 0.35 to 0.399 mm specified in the American Pharmacopoeia Standard [21]. Thus, the present braided sutures are applicable in terms of a tensile strength, which is the most important property for a suture in clinic applications. It is worth mentioning that the coating of chitosan on the PLLA suture resulted in essentially no loss of the tensile strength. In the previous report [14], the unknotted PLLA threads with a diameter of about 0.36 mm exhibited a breaking force of 5.5N, whereas the present PLLA braided wire was more than 60% higher in tensile strength behavior.

In order to further understand whether the developed PLLA braided wire could be sutured inside a body, an animal test was done in this work. Figure 10 shows a picture of suturing of the PLLA braided wire without chitosan coating inside the upper limb muscle of a CD mouse imbedded after 28 days. The figure clearly indicated that the PLLA braided wire displayed preferable suturing effect with a sound knot and the wound was healing up smoothly.

3.4 Hemolytic property

Blood compatibility of the sutures was estimated by their hemolytic ratio (HR). Hemolysis occurs when the blood contacts with surface of a foreign body, as some hematids can be destructed accompanied subsequently with a release of hemoglobin. A material with excellent blood compatibility should have a low hemolysis ratio [22]. High hemolysis might cause internal side effects. It is generally thought that no harmful side effect occurs if a hemolysis ratio is lower than 5% [23]. The measured blood compatibility data are summarized in Table 3**.** It can be seen that both the PLLA and the PLLA-CS sutures had HR values lower than 5%. Specifically, $HR_{PLLA\ suture} = 4.75\%$ while $HR_{ch\text{-}suture} = 4.08\%$. This was because chitosan carried a trace of positive charges on its surface resulting from amino protonation, which is beneficial to the reduction of HR value. When contacted with blood, an electrostatic attraction between chitosan surface and erythrocyte membrane containing anionic glycoproteins induced a curvature on the erythrocyte membrane, which eventually led to a rupture and release of hemoglobin. It is concluded that both the sutures exhibited good blood compatibility [24].

3.5 Kinetic hemostasis

Hemolysis occurs when red blood cells within uncoagulated blood come into contact with water. So, the absorbency of the water reflects the uncoagulated quantity of the blood on contact with the suture. A higher absorbency

Table 2 Tensile property

Sample	Diameter (mm)	Breaking force (N)	Breaking strength (MPa)	Breaking strain (%)	Youngs modules (MPa)
PLLA	0.352 ± 0.007	8.754 ± 0.295	90.000 ± 2.568	83.507 ± 2.722	187.413 ± 10.324
PLLA-CS	0.351 ± 0.008	8.870 ± 0.318	91.720 ± 3.136	90.709 ± 3.785	208.239 ± 14.537

Table 3 The hemolysis experimental results

Sample	$X \pm s(A_{545\ nm})$	HR
A_P	0.764	$4.75\%_{(PLLA)}$
A_N	0.006	
$A_{S/PLLA}$	0.042	$4.08\%_{(PLLA\text{-}CS)}$
$A_{S/PLLA\text{-}CS}$	0.037	

indicated that the solution contained more concentrated hemoglobin, namely, the less blood was coagulated on the surface of the suture. The quicker the absorbency decreased with the time, the shorter the clotting time was, and the better hemostatic effect the materials had.

Figure 11 shows the dynamic blood clotting profiles for two kinds of sutures. The absorbency of the hemolyzed hemoglobin solution decreased with an increased contact time of blood with the samples. In addition, the absorbency of the solution for PLLA-CS suture was decreasing more quickly than that for PLLA suture without chitosan, and approximately near to that for glass sample at 10 min on which the blood coagulation generally occurred after 5 min contact, indicating that the chitosan coated on PLLA suture could induce the blood coagulation and had a good hemostatic property.

3.6 Platelet adhesion

In normal hemostasis, platelets play a crucial role. Plasma protein is absorbed firstly on the surface of materials when blood contacts with the materials, followed by adherence and deformation of the platelets and then startup a cruor process. In addition, the platelets stimulate local activation of the plasma's clotting factors, generating the formation of a fibrin clot that reinforces the platelet aggregates [25, 26]. It has been long recognized that because of poor solubility direct applications of chitin are limited. Hence, a deacetylated product, chitosan, has gained much more attentions in practice. The effect of chitosan on hemostasis is not only due to a physical interaction, but also related with its chemical structure particularly amino residue.

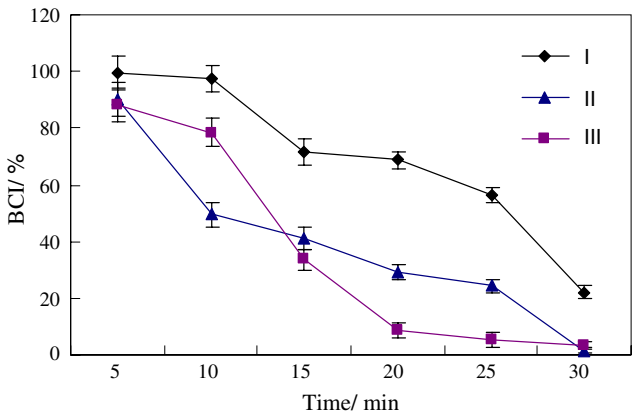

Fig. 11 Dynamic hemostasis process for PLLA suture (I), PLLA-CS suture (II) and a reference glass (III)

The platelet adhesion on each sample was qualitatively assessed based on the morphology of SEM images. Figures 12a, b illustrate the platelets which have contacted with surfaces of the PLLA and PLLA-CS sutures for 30 min, respectively. It was observed that the platelets adhered strongly on the surfaces of both the sutures. Furthermore, the platelets were bound to each other and formed an aggregated mass. The platelets on the PLLA-CS sutures were greater in number than those on the PLLA sutures, but most of the adhered platelets were round with only a few filopodia. This is in consistent with the observations of Janvikul et al. [27], in which they demonstrated that the hydrophilic materials can provide better platelet attachment and activation. Consequently, the PLLA-CS suture of more hydrophilic characteristic is in favor of better platelet adhesion and hemostatic effect. This provides a partial explanation why blood would coagulate quickly on the PLLA-CS suture in a kinetic hemostasis experiment.

3.7 Erythrocyte adhesion

Aggregation of erythrocytes also plays an important role in hemostasis. The adhesion of erythrocyte on each sample was shown in Fig. 13. The erythrocytes adhered strongly on surfaces of both the PLLA and PLLA-CS sutures and formed an aggregation mass. Obviously, the sutures coated with chitosan absorbed more erythrocytes than the ones without chitosan coating. In addition, the erythrocytes on the surface of the plain PLLA sample exhibited a smooth morphology (Fig. 13a), whereas those on the surface of the PLLA-CS sample (Fig. 13b) were seen to possess pseudopodias and were bound to each other in an aggregating form. This indicated that the PLLA-CS attracted and activated the erythrocytes effectively. Okamoto and Malette [16, 28] thought that chitosan could shorten dynamical clotting time, not only due to an effect of platelets but also because of adhesion and activation of the erythrocytes. Hence, it was the introduction of chitosan that brought the results of amidocyanogen [29] or acetyl group [30] with chitosan molecules and dielectric property. Hou [29] recognized that the amidocyanogen of chitosan could neutralize negatively charged neuraminic acid residues, which are located on the surface of erythrocytes. It can be informed that the PLLA-CS suture showed better hemoglutination than the plain PLLA suture because of a dual function of platelets and erythrocytes together with the

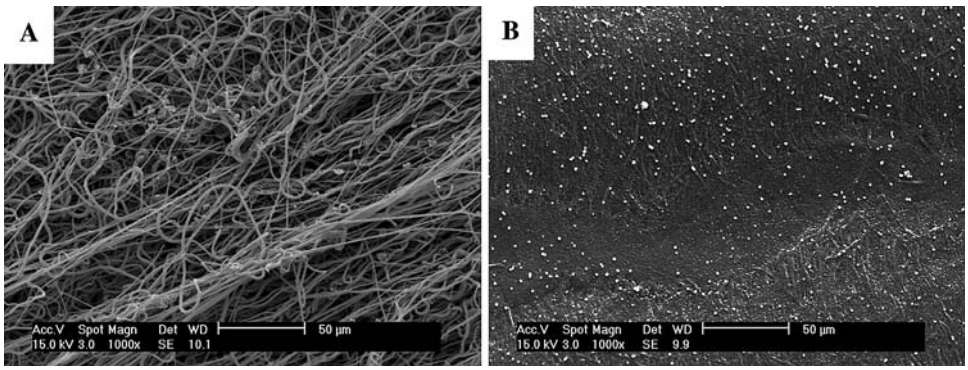

Fig. 12 SEM images of adherent platelets (×1000) on **a** PLLA suture and **b** PLLA-CS suture. Many large aggregates are present on surface of the PLLA-CS suture, and the surface is covered extensively with platelets. The platelets on plain PLLA suture surface show smaller aggregates, but noticeably less adherent platelets which maintain a fairly inactive morphology

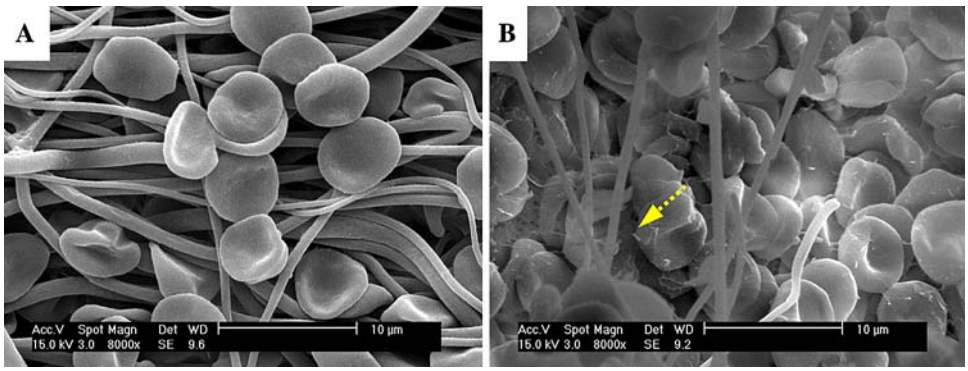

Fig. 13 Morphology of human erythrocytes (×5000) for blood mixed with **a** PLLA suture, **b** PLLA-CS suture. The erythrocytes on the surface of plain PLLA suture shows a smooth morphology while extend pseudopodias of PLLA-CS suture (as *arrow* points)

introduction of chitosan. This could also be used to explain the results in a kinetic hemostasis experiment.

3.8 Water uptake behavior

Water uptake ability of a biomaterial is an important factor for cell seeding, which affects distribution of cell suspension throughout the material and a transfer efficiency of oxygen and nutriment. Figure 14 shows the water uptake abilities of the PLLA suture, PLLA-CS suture, and PLLA suture coated with chitosan three times. It can be seen that the incorporation of chitosan onto the PLLA suture significantly improved its water uptake ability. The water uptake ability of the suture coated with chitosan three times was the highest. Furthermore, the PLLA-CS suture could not only hold more water but also have a quicker water uptake rate. This should be attributed to an excellent hydrophilicity of chitosan itself. On the other hand, as illustrated in Fig. 13, the water uptake of all the samples showed a burst start within 4 h, followed by a slow increase until 24 h. Essentially, the PLLA sutures reached saturation in water uptake for 24 h, but the uptake ability was increased with the incorporation of chitosan. There are several parameters affecting the water uptake ability of a suture, which include hydrophilicity and pore structure of the suture. Due to the incorporation of chitosan, the hydrophilicity of the PLLA-CS suture was greatly improved compared with the pure PLLA suture, whereas the porosity of the PLLA–CS suture was reduced. These resulted in a high water uptake rate especially at the initial stage. It then became steady. In principal, more chitosan incorporated would lead to higher hydrophilicity of the samples and lower porosity on the sutures.

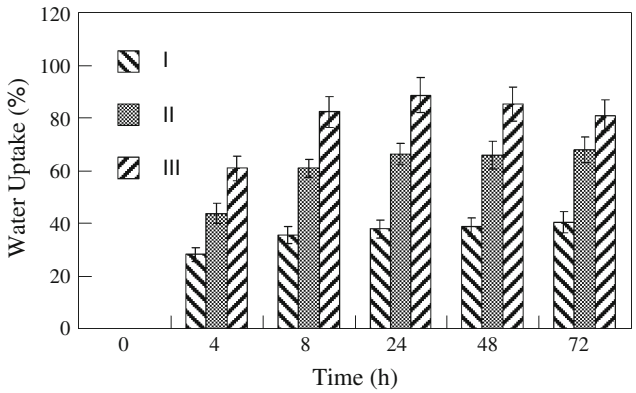

Fig. 14 Water uptake abilities of PLLA suture (I), PLLA-CS suture (II) and PLLA suture coated with chitosan three times (III)

4 Conclusion

Braided ploy (L-lactic) wire suture (PLLA suture) was successfully fabricated by using electrospinning processing followed by a braiding technique. The prepared suture was characterized by SEM, XPS, tensile, and hemostatic tests.

The results shown that the braiding technique significantly increased mechanical performance of an electrospun fiber thread obtained using a sharp-edged rotating disc of a high speed which could gather aligned fibers with a highly ordered structure. It was found that coated with chitosan a thin film was formed on surface of the PLLA suture, and the tensile properties of the suture were essentially not affected by the coating solution of chitosan with acetic acid. The chitosan coated PLLA suture exhibited better blood compatibility, compared with the plain PLLA suture, and had an ability to cause platelet and erythrocyte aggregation. It also displayed superior hemositasis characteristics.

Acknowledgment This research is partially financially supported by the National Natural Science Foundations of China with a grant number of 50773054.

References

1. Chu CC. Textile-based biomaterials for surgical applications. In: Dumitriu S, editor. Polymeric iomaterials. 2nd ed. New York: Marcel Dekker; 2002. p. 167–86.
2. Lee K-H, Chu CC. The role of superoxide ions in the degradation of synthetic absorbable sutures. J Biomed Mater Res. 2000; 49:25–35.
3. Ooi CP, Cameron RE. The hydrolytic degradation of polydioxanone (PDSII) sutures. Part I: morphological aspects. J Biomed Mater Res (Appl Biomater). 2002;63:280–90.
4. Makela P, Pohjonen T, Tormala P, Waris T, Ashammakhi N. Strength retention properties of self-reinforced poly l-lactide (SRPLLA) sutures compared with polyglyconate (Maxons) and polydioxanone (PDS) sutures. An in vitro study. Biomaterials. 2002;23:2587–92.
5. Wissing J, Van Vroonhoven TJMV, Schattenkerk ME, et al. Fascia closure after midline laparotomy: results of a randomized trial. Br J Surg. 1987;74:738.
6. Lewis RT, Wiegand FM. Nature history of vertical abdominal parietal closure: prolene versus dexon. Can J Surg. 1989;32:196.
7. Adekogbe I, Ghanem A. Fabrication and characterization of DTBP-crosslinked chitosan scaffolds for skin tissue engineering. Biomaterials. 2005;26:7241–50.
8. Huang ZM, Zhang YZ, Kotaki M, Ramakrishna S. A review on polymer nanofibers by electrospinning and their applications in nanocomposites. Compos Sci Technol. 2003;63:2223–53.
9. Ramakrishna S, Fujihara K, Teo W-E, et al. Electrospun nanofibers: solving global issues. Mater Today. 2006;9(3):40–50.
10. Khil M-S, Cha D-I, Kim H-Y, et al. Electrospun nanofibrous polyurethane membrane as wound dressing. Mater Res B: Appl Biomater. 2003;67(2):675–9.
11. Katti DS, Robinson KW, Ko FK, et al. Bioresorbable nanofiber-based systems for wound healing and drug delivery: optimization of fabrication parameters. Mater Res B: Appl Biomater. 2004; 70(2):286–96.
12. Huang ZM, He CL, Yang AZ, Zhang YZ, Han XJ, Yin JL, et al. Encapsulating drugs in biodegradable ultrafine fibers through co-axial electrospinning. J Biomed Mater Res. 2006;77A(1):169–79.
13. Barie PS. Surgical site infections: epidemiology and prevention. Surg Infect. 2002;3(S1):9–21.
14. He CL, Huang ZM, Han XJ. Fabrication of drug loaded electrospun aligned fibrous threads for suture applications. J Biomed Mater Res A. 2009;89A(1):80–95.
15. Haas DW, Kaiser AB. Antimicrobial prophylaxis of infections associated with foreign bodies. In: Waldvogel FA, Bisno AL, editors. Infections associated with indwelling medical devices. 3rd ed. Washington, DC: ASM Press; 2000.
16. Malette WG, William G, Quigley HJ, et al. Method of achieving hemostasis. US Patent 4394373. 6 July 1983.
17. Klokkevold PR, Lew DS, Ellis DG, Bertolami CN. Effect of chitosan on lingual hemostasis in rabbits. J Oral Maxillofac Surg. 1991;49:858–63.
18. Klokkevold PR, Subar P, Fukayama H, Bertolami CN. Effect of chitosan on lingual hemostasis in rabbits with platelet dysfunction induced by epoprostenol. J Oral Maxillofac Surg. 1992;50:41–5.
19. ASTM D 2256-02: Standard test methods for testing properties of yarns by the single-strand method, ASTM International. ASTM: West Conshohocken, PA; 2000.
20. Lawrie G, Keen I, Drew B, et al. Interactions between alginate and chitosan biopolymers characterized using FTIR and XPS. Biomacromolecules. 2007;8:2533–41.
21. USP 30-NF 25, Absorbable surgical suture.
22. Zobel HP, Stieneker F, Atmaca-Abdel Aziz S. Evaluation of aminoalkylmethacrylate nanoparticles as colloidal drug carrier systems. Part 2. characterization of antisense oligonucleotides loaded copolymer nanoparticles. J Pharm Biopharm. 1999;48:1.
23. Hou C, Yuan Q, Huo D, Zheng S, Zhan D. Investigation on clotting and hemolysis characteristics of heparin-immobilized polyether sulfones biomembrane. J Biomed Mater Res. 2008;85A:847–52.
24. Yang YD, Yu JG, Zhou YG, et al. Preparation and blood compatibility of oxidized-chitosan films. Chin Chem Lett. 2005;16 (7):991–4.
25. Bick RL. Clinical evaluation of the patient with hemorrhage. In: Bick RL, Bennett J, Brynes R, et al., editors. Hematology: clinical and laboratory practice; vol 2. Mosby: St. Louis, MO; 1993. p. 1285.
26. Bithell, TC. The physiology of primary hemostasis. In: Lee GR, et al., editors. Wintrobe's Clinical Hematology. vol 1. Lea & Febiger: Philadelphia; 1993. p. 540.
27. Janvikul W, Uppanan P, Thavornyutikarn B, Krewraing J, Prateepasen R. In vitro comparative hemostatic studies of chitin, chitosan, and their derivatives. J Appl Polym Sci. 2006;102:445–51.
28. Okamoto Y, Yano R, Miyatake K, et al. Efects of chitin and chitosan on blood coagulation. Carbohydr Polym. 2003;53(3): 337–42.
29. Hou CL, Gu QS. Chitin and medicine. Shanghai: The Shanghai Science and Technology Press; 2001. p. 58–61.
30. Lee KY, Ha WS, Park WH. Blood compatibility and biodegradability of partially N-acylated chitosan derivatives. Biomaterials. 1995;16:1211–6.